Supplementary Information (SI) for Journal of Materials Chemistry C.

Supplementary information for

Mid-infrared bifunctional high-*Q* plasmonic metasurfaces with strong intrinsic chirality and imaging-based biosensing

HAN-LEI XU,[1] ZI-MING MENG,[1,2,3,*] YUAN-HAO LIU,[1] JIN-YUE SU,[1] ZE-ZHOU FANG,[1] AND JIN-YUN ZHOU,[1,2,3]

[1]*School of Physics and Optoelectronic Engineering, Guangdong University of Technology, Guangzhou 510006, China*

[2]*Guangdong Provincial Key Laboratory of Sensing Physics and System Integration Applications, Guangdong University of Technology, Guangzhou, 510006, China*

[3]*Guangdong Provincial Key Laboratory of Information Photonics Technology, Guangdong University of Technology, Guangzhou 510006, China*

**Corresponding author: *mengzm@gdut.edu.cn*

Supplementary note 1: Discussion on metasurface material

In this paper, gold (Au) is chosen as the chiral metasurface material due to its low intrinsic loss, superior chemical stability in the mid-infrared band, and well-established research foundation in chiral optics. The alternative lower-loss metals at mid-infrared band, such as Argentum (Ag) and Natrium (Na) also are considered. However, the performance of chiral metasurface may be significantly affected due to their inferior stability. Additionally, non-noble metals such as copper (Cu) and aluminum (Al) exhibit high optical losses and inadequate chemical stability. Here, Au[1], Ag[2] and Na[3] are employed as metasurface materials, comparing their The real(εr) and imaginary parts(εi) of the relative permittivity as illustrated in the figure S1(a), and comparing their optical chiral responses as illustrated in the figure S1(b). Considering the aspects of Q-factor, circular dichroism and stability, Au demonstrates superior performance as the material of choice.

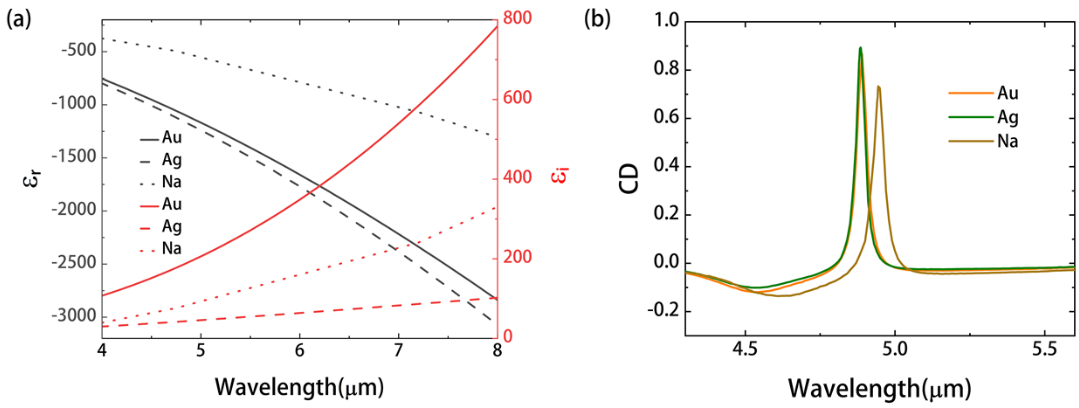

Figure S1 (a) The real and imaginary parts of the relative permittivity of Au, Na, Ag. (b) Optical chiral responses of Au, Ag, Na metasurface.

Supplementary note 2: Discussion on thickness of the protein layer

In this work, the thickness of the protein layer is chosen to 20 nm[4]. We simulated the reflection spectra of metasurfaces (S=1.2) with protein thicknesses ranging from 10 to 50 nm. As shown in Figure S2, increasing protein thickness reduces reflection due to enhanced absorption and induced resonant wavelength redshift. When the protein thickness increases to 100 nm, the resonance mode exhibits a significantly broadened linewidth and degraded Q-factor (though this is not illustrated in the figure), indicating an optimal thickness range of 10-50 nm.

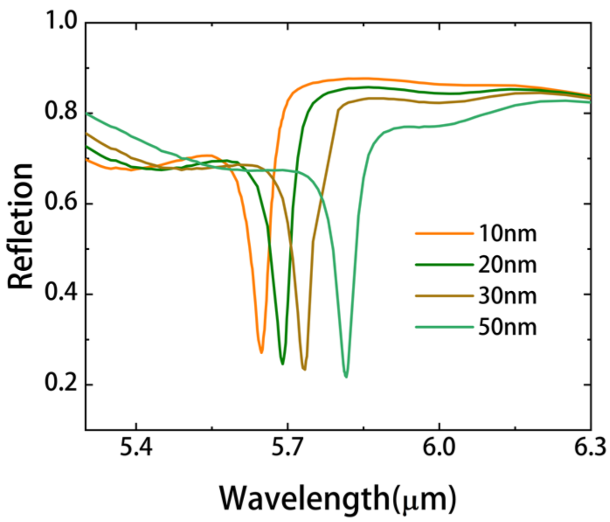

Figure S2 Simulated reflection spectra of metasurfaces with protein thicknesses ranging from 10 to 50 nm.

Supplementary note 3: Discussion on possible fabrication procedure

The proposed metasurface can be fabricated through advanced nanophotonic fabrication technology. The possible fabrication procedure can be elaborated as shown in Figure S3. Firstly, a SiO_2 layer is firstly deposited on Au substrates via PECVD[5]. Then the step-shaped unit cells are firstly built by a series of processes including gray-scale Lithography[6], gold deposition and etching. Finally, the sample will be acquired after the residual resist removal.

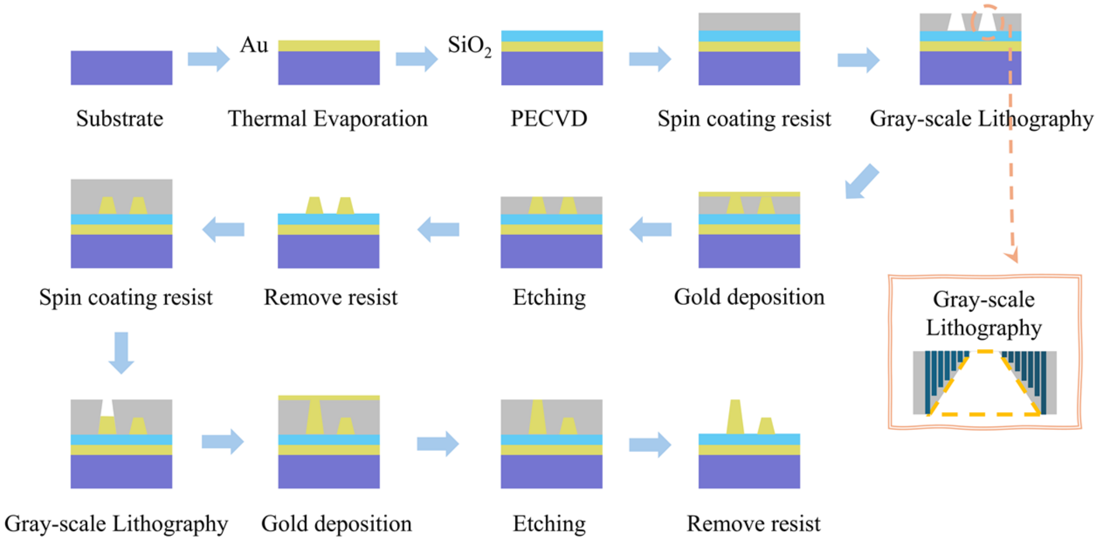

Figure S3 The possible fabrication procedure of proposed metasurface.

Reference

1. R. L. Olmon, B. Slovick, T. W. Johnson, D. Shelton, S.-H. Oh, G. D. Boreman and M. B. Raschke, *Phys. Rev. B*, 2012, **86**, 235147.
2. H. U. Yang, J. D'Archangel, M. L. Sundheimer, E. Tucker, G. D. Boreman and M. B. Raschke, *Phys. Rev. B*, 2015, **91**, 235137.
3. R. Althoff and J. H. Hertz, *Infrared Physics*, 1967, **7**, 11-16.
4. C. D. Tao, C. B. Liu, Y. L. Li, L. J. Qiao, J. Zhou and Y. Bai, *J. Mater. Chem. C*, 2023, **11**, 7068-7075.
5. Y. Q. Hu, Y. T. Jiang, Y. Zhang, X. Yang, X. N. Ou, L. Li, X. H. Kong, X. S. Liu, C. W. Qiu and H. G. Duan, *Nat. Commun.*, 2023, **14**, 9.
6. X. J. Xiao, Y. W. Zhao, X. Ye, C. Chen, X. M. Lu, Y. S. Rong, J. H. Deng, G. X. Li, S. N. Zhu and T. Li, *Light-Sci. Appl.*, 2022, **11**, 9.